

Article

# Fate of Diclofenac and Its Transformation and Inorganic By-Products in Different Water Matrices during Electrochemical Advanced Oxidation Process Using a Boron-Doped Diamond Electrode

Carolin Heim<sup>1,2</sup>, Mohamad Rajab<sup>1</sup>, Giorgia Greco<sup>1</sup>, Sylvia Grosse<sup>1</sup>, Jörg E. Drewes<sup>1</sup>, Thomas Letzel<sup>1,3</sup> and Brigitte Helmreich<sup>1,\*</sup> 

<sup>1</sup> Chair of Urban Water Systems Engineering, Technical University of Munich, Am Coulombwall 3, 85748 Garching, Germany; c.heim@tum.de (C.H.); ragabco@gmail.com (M.R.); greco.chem@gmail.com (G.G.); grossesylvia@hotmail.com (S.G.); jdrewes@tum.de (J.E.D.); t.letzel@tum.de (T.L.)

<sup>2</sup> Institute of Pharmacology and Toxicology, Technical University of Munich, Biedersteiner Str. 29, 80802 Munich, Germany

<sup>3</sup> Analytisches Forschungsinstitut für Non-Target Screening GmbH, Am Mittleren Moos 48, 86167 Augsburg, Germany

\* Correspondence: b.helmreich@tum.de; Tel.: +49-89-289-13719

Received: 9 May 2020; Accepted: 9 June 2020; Published: 12 June 2020



**Abstract:** The focus of this study was to investigate the efficacy of applying boron-doped diamond (BDD) electrodes in an electrochemical advanced oxidation process, for the removal of the target compound diclofenac (DCF) in different water matrices. The reduction of DCF, and at the same time the formation of transformation products (TPs) and inorganic by-products, was investigated as a function of electrode settings and the duration of treatment. Kinetic assessments of DCF and possible TPs derived from data from the literature were performed, based on a serial chromatographic separation with reversed-phase liquid chromatography followed by hydrophilic interaction liquid chromatography (RPLC-HILIC system) coupled to ESI-TOF mass spectrometry. The application of the BDD electrode resulted in the complete removal of DCF in deionized water, drinking water and wastewater effluents spiked with DCF. As a function of the applied current density, a variety of TPs appeared, including early stage products, structures after ring opening and highly oxidized small molecules. Both the complexity of the water matrix and the electrode settings had a noticeable influence on the treatment process's efficacy. In order to achieve effective removal of the target compound under economic conditions, and at the same time minimize by-product formation, it is recommended to operate the electrode at a moderate current density and reduce the extent of the treatment.

**Keywords:** advanced water treatment; by-product formation; electrochemical oxidation; energy demand; micropollutants; operation conditions; oxidation products

## 1. Introduction

The growing consumption of pharmaceuticals worldwide is resulting in an increasing threat to human health and the aquatic environment, as many of these polar and semi-polar micropollutants are not removed, or only incompletely removed, by traditional biological treatment technologies in wastewater treatment plants [1]. Advances made in environmental analytical chemistry have made it possible to monitor such persistent pollutants in water bodies, such as surface and groundwater, in wastewater effluents, and in drinking water at very low levels [2–5].

Among the large variety of pharmaceutical compounds present in the environment, the non-steroidal anti-inflammatory drug diclofenac (DCF) is one of the most-consumed substances; the annual intake worldwide is estimated to exceed 1000 tons [6]. The annual consumption of DCF per capita varies between 195 and 940 mg [5]. DCF is known to be highly soluble in water. Its log  $K_{ow}$  value of 4.5–4.8 suggests a potential for adsorption into mixed liquor during wastewater treatment. However, at a pH value above its  $pK_a$  of 4.0–4.5, the carboxyl group of DCF dissociates and the molecule becomes negatively charged, exhibiting a lower tendency to adsorb into sludge (Log  $k_D$ : 1.2–2.1). Additionally, DCF is only moderately biodegradable under suboxic and anoxic conditions ( $k_{biol}$ :  $\leq 0.1$  L/g·day) [5–7]. Thus, conventional wastewater treatment, as summarized by Lonappan et al., is limited due to these properties [6]. Other technologies, such as ozonation, membrane filtration methods or adsorption in activated carbon, are highly effective against DCF, but are also cost-intensive [3,8].

DCF has been detected in effluents of wastewater treatment plants (WWTPs) in concentrations of up to 10  $\mu\text{g/L}$ , in surface (up to 15  $\mu\text{g/L}$ ) and in groundwater (up to 0.15  $\mu\text{g/L}$ ), and in drinking water in the low ng/L range [5,8–11]. In combination with other drugs present in the water, the toxicity of DCF was reported to increase considerably [10–13]. Due to the demonstrated risk to the aquatic environment, the European Union (EU) considered emerging contaminants, and put DCF on the first watchlist for monitoring [14]. In addition, environmental quality standard values of 0.1  $\mu\text{g/L}$  for inland waters and 0.010  $\mu\text{g/L}$  for coastal waters were proposed for DCF [14,15].

Nowadays, researchers are seeking new and efficient technologies to improve the situation, resulting in innovative and low-cost alternatives for the treatment of drinking water and post-treatment of wastewater effluents. In recent years, advanced oxidation processes (AOPs) have gained attention as very effective technologies in the oxidation of numerous organic micropollutants [16–18]. AOPs are based on the generation of free radicals, mainly the hydroxyl radical with high oxidizing power, which can successfully attack most organic molecules with elevated reaction constants ranging from  $10^6$  to  $10^{10}$   $\text{M}^{-1}\text{s}^{-1}$  (e.g., [19,20]). Regarding the method for generating hydroxyl radicals, AOPs are divided into four groups: chemically (e.g.,  $\text{O}_3/\text{H}_2\text{O}_2$ ;  $\text{H}_2\text{O}_2/\text{Fe}^{2+/3+}$  (Fenton)), sono-chemically (e.g.,  $\text{H}_2\text{O}_2/\text{ultrasonic}$ ), photo-chemically (e.g.,  $\text{H}_2\text{O}_2/\text{UV}$ ;  $\text{H}_2\text{O}_2/\text{UV}/\text{Fe}^{2+/3+}$  (Photo-Fenton)) and electrochemically [e.g., boron-doped diamond electrodes (BDD)] [18,21–24]. A variety of advanced treatment methods, such as application of UV or UV/ $\text{H}_2\text{O}_2$ , radiation, ozonation, sonolysis and electrochemical treatment, has been discussed by Schröder et al., regarding their efficiency in degrading DCF in different water sources [5]. Most of these technologies require cost-intensive chemicals, have to overcome environmental and safety issues, or have to apply energy-rich filtration or irradiation. The advantages of electrochemical AOPs are based on their in situ generation of a variety of oxidants under economically and environmentally friendly conditions [5].

The application of BDD in electrochemical AOP has been successful in the removal of a variety of organic pollutants from water and wastewater. Several studies relate to the effectiveness of DCF treatment using BDD electrodes [11,25–28]. Due to the inertness of the diamond, the chemical stability and the high oxygen evolution overpotential, these electrodes show high treatment efficiencies compared to other materials [17,19,25–32]. Depending on the water composition, various oxidative species, such as hydroxyl radicals, hydrogen peroxide, ozone and eventually chlorine-based compounds, are responsible for the transformation of the target compounds using BDD [28,32–35]. In general, there is no mineralization during oxidative treatment under realistic conditions [36]. However, oxidants can also carry out reactions with other organic water constituents, which result in the formation of sometimes-toxic by-products, such as bromate and chlorate [37]. In addition, transformation products with a higher toxicity than the parent compound can be generated during the oxidative treatment of micropollutants, as observed in the photocatalytic degradation of DCF [38] as well as N-oxides via treatment with ozone [9,39,40]. So far, the degradation of DCF and production of possible transformation products (TPs), as well as of unwanted inorganic by-products, may be quite heterogeneous, due to competitive reactions with organic and inorganic constituents at high concentrations in drinking water and WWTP effluents [23,41].

The aim of this study was to characterize the oxidative degradation process of DCF as a model target, including assessment of the kinetics, the formation of organic TPs and inorganic by-products, and the energy consumption in water matrices with increasing complexity. This approach allows for the first time a comprehensive examination of DCF degradation, as an exemplary persistent pollutant in electrochemical water treatment, linking DCF transformation with by-product formation and energy expenditure. For this purpose, DCF was spiked into deionized water, synthetic hard drinking water and a real wastewater effluent, and treated using a BDD electrode under varying electrode settings. Based on the generated data, the extent of oxidation and possible optimization steps of the process, with respect to minimizing potentially unwanted by-products and the specific energy demand, are topics of discussion.

## 2. Materials and Methods

### 2.1. Chemicals

Sodium hydroxide (NaOH), sodium sulfite (Na<sub>2</sub>SO<sub>3</sub>), phosphoric acid (H<sub>3</sub>PO<sub>4</sub>), calcium chloride (CaCl<sub>2</sub>), potassium bromide (KBr), potassium iodide (KI), magnesium sulphate heptahydrate (MgSO<sub>4</sub> · 7H<sub>2</sub>O), sodium hydrogen carbonate (NaHCO<sub>3</sub>) and sodium nitrate (NaNO<sub>3</sub>) were purchased from Merck (Darmstadt, Germany). DCF was purchased from Sigma-Aldrich Chemie (Steinheim, Germany), acetonitrile HiPerSolv Chromanorm from BDH Chemicals Limited (Poole, UK). Water LC-MS Chromasolv (for liquid chromatography use) was bought from Fluka (Buchs, Switzerland). Ammonium acetate (CH<sub>3</sub>COONH<sub>4</sub>) was purchased from Sigma-Aldrich (Seelze, Germany), fumaric acid, oxalic acid, metha- and para-hydroxybenzoic acids from Sigma (Deisenhofen, Germany), and maleic acid from SERVA (Heidelberg, Germany), and these were used as standard chemicals for LC-MS/MS analysis. All chemicals were of analytical-reagent grade.

### 2.2. Water Matrices

Experiments were conducted in three water matrices: (a) deionized water (deionizer “Milli-Q Plus 185”); (b) synthetic hard drinking water; and (c) a wastewater effluent collected from the municipal WWTP Garching, Germany (31,000 population equivalents, two-step aerobic biological treatment). Concentrations of organic and inorganic water constituents and other relevant parameters are summarized in Table 1. Each water matrix was spiked with DCF to reach a final concentration of 50 µM.

**Table 1.** Concentrations of the water constituents and measured parameters in the water matrices.

Parameter	Unit	Deionized Water	Hard Drinking Water	Wastewater Effluent
chloride	mg/L	n.d.	250	180 ± 10
bromide	mg/L	n.d.	1.0	<0.5
nitrate	mg/L	n.d.	50.0	48.5
sulfate	mg/L	n.d.	200	45.4
iodide	mg/L	n.d.	0.1	n.d.
DOC	mmol/L	n.d.	3.6	12.0
pH	-	5.5	8.9	8.0
el. conductivity	µS/cm	0.06	1230	1170

DOC: dissolved organic carbon, n.d.: not detected.

### 2.3. Experimental Setup and Sampling

Experiments were conducted with a CONDIAPURE<sup>®</sup> test system (CONDIAS GmbH, Itzehoe, Germany) using a DIACHEM<sup>®</sup> electrode stack (CONDIAS, Itzehoe, Germany). The stack consisted of a single anode/cathode pair of niobium, coated with a 5- to 7-µm-thick boron-doped diamond layer with an electrode surface of 24 × 50 mm<sup>2</sup> per electrode. A nafion cation exchange membrane was

placed in direct contact with the cathode and anode in order to create a gap-free sandwich structure and thus enhance the current density locally, which promoted ozone formation [19]. The electrode stack was integrated into an optically accessible glass reactor (Esau & Hueber GmbH, Schrobenuhausen, Germany). The experimental setup has been described elsewhere [31,42]. Three liters of DCF solution of each water matrix were prepared in a glass vessel (tempered to  $20\text{ }^{\circ}\text{C} \pm 1\text{ }^{\circ}\text{C}$ ), which was connected to the operation unit with an inlet and outlet tube. The reaction solution was circulated through the glass reactor by a centrifugal pump (PY-2071, Speck Pumpen, Hilpoltstein, Germany) at a flow rate of 4 L/min. Electrolytic treatment was carried out for an overall time of 30 min for deionized water, and 60 min for drinking water and wastewater, using current densities of  $j = 42, 167$  and  $292\text{ mA/cm}^2$ , respectively. Electricity consumption was monitored using the Energy Monitor 3000 (Votcraft, Hirschau, Germany).

Samples (2 mL each) were collected directly from the glass vessel after a period of 0, 1, 2, 3, 5, 7.5, 10, 15, 20, 30 and 60 min. The oxidation reaction in the samples was terminated by adding 20  $\mu\text{L}$  of 10 mM  $\text{Na}_2\text{SO}_3$  directly after sampling. Samples were subsequently filtered through 0.22  $\mu\text{m}$  polyvinylidene fluoride (PVDF) Pleomax filters before the analysis of DCF and TPs.

#### 2.4. Analysis

DCF and TPs were analyzed with two-dimensional liquid chromatography (LC) by serial coupling of reversed-phase liquid chromatography with hydrophilic interaction liquid chromatography (RPLC-HILIC) and an electrospray ionization time-of-flight mass spectrometer (ESI-TOF-MS).

Oxidation mixtures were injected on a serial RPLC-HILIC-ESI-TOF-MS system containing two Agilent HPLC systems series 1260 Infinity (Waldbronn, Germany) coupled to an Agilent TOF-MS system series 6230 with Jet Stream ESI interface (Agilent Technologies, Santa Clara, CA, USA). Chromatographic separation was performed by serial coupling of a Poroshell 120 EC-C18 column ( $50.0\text{ mm} \times 3.0\text{ mm}$ ,  $2.7\text{ }\mu\text{m}$ ) (Agilent Technologies, Santa Clara, CA, USA) and a ZIC<sup>®</sup>-HILIC column ( $150\text{ mm} \times 2.1\text{ mm}$ ,  $5\text{ }\mu\text{m}$ ,  $200\text{ \AA}$ ) (Merck Sequant, Umeå, Sweden) based on a method described by Greco et al. [43]. Injection volume was 10  $\mu\text{L}$ . The RPLC mobile phase was a mixture of ammonium acetate 10 mM/acetone nitrile (90:10, v/v) and ammonium acetate 10 mM/acetone nitrile (10:90, v/v) at a flow rate of 0.1 mL/min. The HILIC mobile phase was a composition of acetone nitrile, water and the solvent from the RP column at a flow rate of 0.4 mL/min. The Jet Stream ESI source was used in negative mode with the conditions described elsewhere [23]. The HPLC systems, the ESI interface and the mass spectrometric detector were controlled and data were acquired and processed by MassHunter software (Agilent Technologies, Waldbronn, Germany) using the extraction ion chromatogram (EIC) technique within a maximum mass tolerance of 10 ppm. The accurate mass data of the TPs were processed as previously described by Stadlmair et al. [44].

The pH value was controlled based on Standard Method 4500-H<sup>+</sup> [45]. Ozone concentrations were quantified as residual ozone by photometric measurement at 610 nm after decolourization of indigo bisulfonate based on the descriptions given by Bader and Hoigné [46] with modifications described before [47]. Instead of phosphate buffer, phosphoric acid was employed. Concentrations of the inorganic ions chloride ( $\text{Cl}^-$ ) and bromide ( $\text{Br}^-$ ) as well as chlorate ( $\text{ClO}_3^-$ ) and perchlorate ( $\text{ClO}_4^-$ ) were analyzed by ion chromatography with a DIONEX ICS-1000 device (Thermo Scientific Dionex, Sunnyvale, CA, USA) according to Standard Method 4110 [45]. Detection limits for  $\text{Br}^-$ ,  $\text{Cl}^-$  and  $\text{ClO}_3^-$  were 0.05 mg/L in deionized water, and 0.5 mg/L in drinking water and wastewater effluent, respectively.  $\text{ClO}_4^-$  could be detected to 0.1 mg/L in deionized water and 1 mg/L in drinking water and wastewater effluent. Additionally, formation of  $\text{ClO}_3^-$  and  $\text{ClO}_4^-$  as well as the inorganic by-products bromate ( $\text{BrO}_3^-$ ) and perbromate ( $\text{BrO}_4^-$ ) was analyzed semi-quantitatively with RPLC-HILIC-ESI-TOF-MS as described above.

### 3. Results and Discussion

#### 3.1. Removal of Diclofenac

BDD electrodes generate hydroxyl radicals at the anode surface from water molecules.



In subsequent reactions, other oxidants, such as ozone, hydrogen peroxide and further radical species as well, are formed [48,49]:



In complex water matrices, using chlorine-containing molecules, a variety of reactive molecules, including active chlorine species, can also arise. At the BDD electrode, the amounts of oxidants increase when applying higher current densities [49,50].

The electrochemical oxidation of DCF with a BDD electrode was investigated, following procedures reported in a previous study [23]. For this purpose, DCF was spiked at a concentration of 50  $\mu\text{M}$  into the three different water matrices of deionized water, drinking water and wastewater effluent. These water matrices were treated with different current densities  $j$  of 42, 167 and 292  $\text{mA}/\text{cm}^2$ , respectively. Degradation of DCF over the applied cumulative current per volume, expressed as %-variation of the peak area of the respective EIC, for the three water matrices is displayed in Figure 1.

The degradation of DCF in deionized water (Figure 1a) was almost identical for the three applied current densities, with a relatively quick removal of the parent compound. Complete degradation of DCF could be achieved within approximately 350  $\text{mAh}/\text{L}$  (cumulative charge input at a certain reaction time, depending on the respective reactor volume) at 167  $\text{mA}/\text{cm}^2$ , which corresponds to a treatment time of 30 min. Applying 292  $\text{mA}/\text{cm}^2$ , or around 310  $\text{mAh}/\text{L}$ , was required for complete elimination of the target compound. At the lowest current density, the maximum removal level was around 40%, as the cumulative current per volume (93  $\text{mAh}/\text{L}$ ) was not sufficient for complete elimination of DCF. Thus, the degradation did not depend on the applied current density, and required a total current per volume of approximately 310  $\text{mAh}$ , which was not achieved for the lowest current density within the applied treatment time.

In drinking water (Figure 1b), complete degradation could be observed after approximately 450  $\text{mAh}/\text{L}$  for both higher current densities, whereas using 42  $\text{mA}/\text{cm}^2$  resulted in a significantly slower DCF degradation, with a maximum removal rate of 30% at 195  $\text{mAh}/\text{L}$ . In wastewater effluent (Figure 1c), application of 292  $\text{mA}/\text{cm}^2$  resulted in the highest slope of all degradation experiments, but the results did not vary much from using 167  $\text{mA}/\text{cm}^2$ . Complete removal of the compound required approximately 670  $\text{mAh}/\text{L}$ , which could be achieved at 292  $\text{mA}/\text{cm}^2$ . The variation between both curves at 292  $\text{mA}/\text{cm}^2$  and 167  $\text{mA}/\text{cm}^2$ , from 400  $\text{mAh}/\text{L}$  onwards, might derive from the fact that at different current densities, samples were not taken at the same  $Q/V$  values, as sampling was time-dependent. Thus, the progress of the curves, from 400  $\text{mAh}/\text{L}$  until complete degradation of DCF, can only be estimated. Degradation experiments for the lowest current density in wastewater effluent resulted in a significantly lower degradation rate of only up to 25%, compared to the higher current densities. Therefore, the removal of DCF in wastewater effluents under 42  $\text{mA}/\text{cm}^2$  is not feasible.

The observed variations in DCF removal between the different water matrices are most likely caused by the presence of competing inorganic and organic compounds in the complex water matrices, which generally reduce the availability of hydroxyl radicals and ozone, as those compounds scavenge the oxidizing agents and therefore lower the degradation rates of the target compound [2,37,51].

In the case of deionized water, there is no competition between target molecules and other inorganic and organic components, leading to a maximum efficiency of DCF removal. The drinking water contained inorganic ions in relatively high concentrations, which extended the overall treatment process. The additional presence of organic compounds in the wastewater effluent (at lower concentration of inorganic compounds compared to the drinking water) further prolonged the electrochemical oxidation process until complete removal of DCF. Overall, the impact of inorganic constituents, in particular chloride, nitrate and sulfate, on DCF transformation during BDD treatment was more noticeable than the competition between the target compound and organic matter, which strongly depends on the respective concentrations in the water matrix.

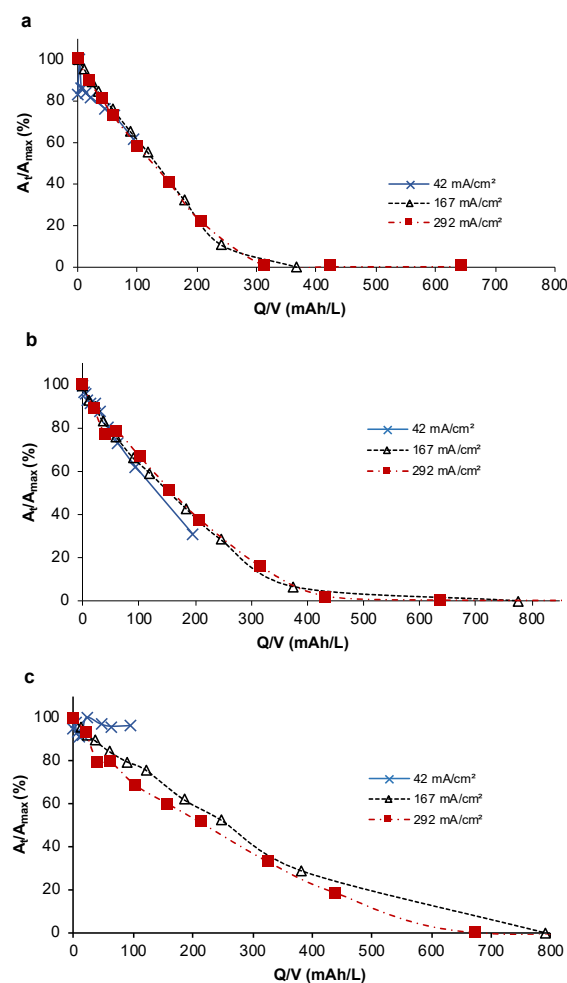


**Figure 1.** Degradation of diclofenac (DCF) expressed as %-variation of the peak area ( $A_t/A_{max}$ ) of the respective EIC over the applied charge per volume ( $Q/V$ ) in deionized water (a), drinking water (b), and wastewater effluent (c), at three different current densities ( $j = 42, 167$  and  $292$  mA/cm<sup>2</sup>).

DCF reacts with both ozone and hydroxyl radicals, as both can be formed by the BDD electrode used in this study [31]. The reaction constants for the oxidation of DCF with non-selective hydroxyl radicals ( $k_{OH} 7.5 \pm 1.5 \times 10^9$  M<sup>-1</sup>s<sup>-1</sup>) are higher than those with ozone ( $k_{O_3}$  around  $1 \times 10^6$  M<sup>-1</sup>s<sup>-1</sup>) [2,37]. As the compound is showing a good, selective reactivity towards ozone [41], it is possible to monitor the matrix-driven depletion of oxidants through the measurement of dissolved ozone in the different water matrices. The maximum ozone values in drinking water were 0.068 mg/L for 42 mA/cm<sup>2</sup>, 0.354 mg/L for 167 mA/cm<sup>2</sup>, and 1.07 mg/L for 292 mA/cm<sup>2</sup>. In wastewater effluent, the highest values were significantly lower, resulting in 0.022 mg/L at 42 mA/cm<sup>2</sup>, 0.185 mg/L at 167 mA/cm<sup>2</sup> and 0.553 mg/L at 292 mA/cm<sup>2</sup>.

Non-selective oxidation is present through hydroxyl radicals, and selective oxidation through ozone and chlorine species (in complex water matrices). In complex water matrices containing chloride ions, the formation of hypochlorite, chlorine dioxide and other chlorine-containing reactive oxygen species is also possible. Since active chlorine species are highly reactive (but less effective compared to ozone) towards DCF (reaction constant  $k_{\text{ClO}_2} = 1.05 \times 10^4 \text{ M}^{-1}\text{s}^{-1}$ ,  $k_{\text{Cl}_2} = 3.89 \pm 1.17 \text{ M}^{-1}\text{s}^{-1}$ ), the electrochemical treatment of DCF can be highly effective in water with high chloride concentrations, through the release of chlorine compounds resulting from the oxidation of DCF. Oxidant concentrations increase with the applied current density. However, other critical inorganic by-products, such as chlorate and perchlorate, arise during the process [2,51–53], which is discussed later in this study.

Since electro-oxidation with BDD electrodes produces a mixture of oxidants, including ozone and hydroxyl radicals, it is possible to combine the selective and non-selective degradation of the parent compound and generated TPs. For DCF with a high reactivity towards ozone, this combination seems to be ideal for achieving a complete removal of the target compound. Vogna et al. [54] reported a complete decomposition of DCF (initial concentration 1 mM) after 8 min of treatment, by introducing an initial ozone concentration of 48 mg/L of ozone in the gas phase into deionized water. In the present study, concentrations of residual dissolved ozone in deionized water were measured at a maximum of 1.8 mg/L, using the highest current density of 292 mA/cm<sup>2</sup>. Initial ozone concentrations, however, could not be examined during the experiment.

In the present study, residual ozone concentrations in the chloride-containing drinking water were significantly lower than those in deionized water. DCF degradation, however, appeared comparable within those two matrices. Initial degradation of DCF was faster in drinking water, most likely caused by oxidants arising from high chlorine concentrations. In wastewater effluent, other organic compounds could also react with active chlorine species, resulting in prolonged DCF degradation time.

Apparently, the effect of oxidant depletion through the high concentrations of the inorganic and organic constituents of wastewater effluent is predominant at the lowest current density. In this case, the formation of ozone can be neglected, and oxidation through hydroxyl radicals is instead driven by mass transport [35], leading to competitive reactions between the target molecule and other water constituents. This effect is represented by the low degradation rate at 42 mA/cm<sup>2</sup>, which differs significantly from the higher current densities. In drinking water with a certain content of inorganic constituents, the ratio of hydroxyl radicals and ozone depleted through water matrix components was less noticeable. Thus, the organic matter fraction of wastewater effluent is likely to be the major hydroxyl radical scavenger, which further represses ozone formation at low current densities. Lee et al. [51] reported that hydroxyl radicals are likely to be consumed by any water component in the wastewater matrix.

### 3.2. Formation and Fate of Transformation Products

DCF removal will also result in the simultaneous generation of DCF TPs. These compounds can arise through chemical reactions between the parent compound and other TPs with oxidants, or after chemical reactions such as de-chlorination, de-carboxylation and the cleavage of molecules. During electrolysis in deionized water under the present electrode conditions, TPs from reactions with the main oxidants' hydroxyl radicals and ozone can be expected.

In more complex water matrices, other oxidative species formed during BDD treatment, such as chlorine and hypochlorite, might play a major role in the generation of TPs. Thus, possible TPs were derived from the literature's data based on the oxidation reactions of DCF during ozonation [9,12], as well as the degradation through hydroxyl radicals using photo-Fenton [13,54], through photocatalysis/TiO<sub>2</sub> [38], through BDD treatment [11,25,55] and through chlorination [53]. The list derived from this literature search included 47 known compounds (see [23]) with chemical structures including two aromatic ring systems, one aromatic ring and linear structures. The formation and degradation of these organic oxidation by-products was compared for the different water matrices. Selected identified TPs are summarized in a degradation scheme in Figure 2.

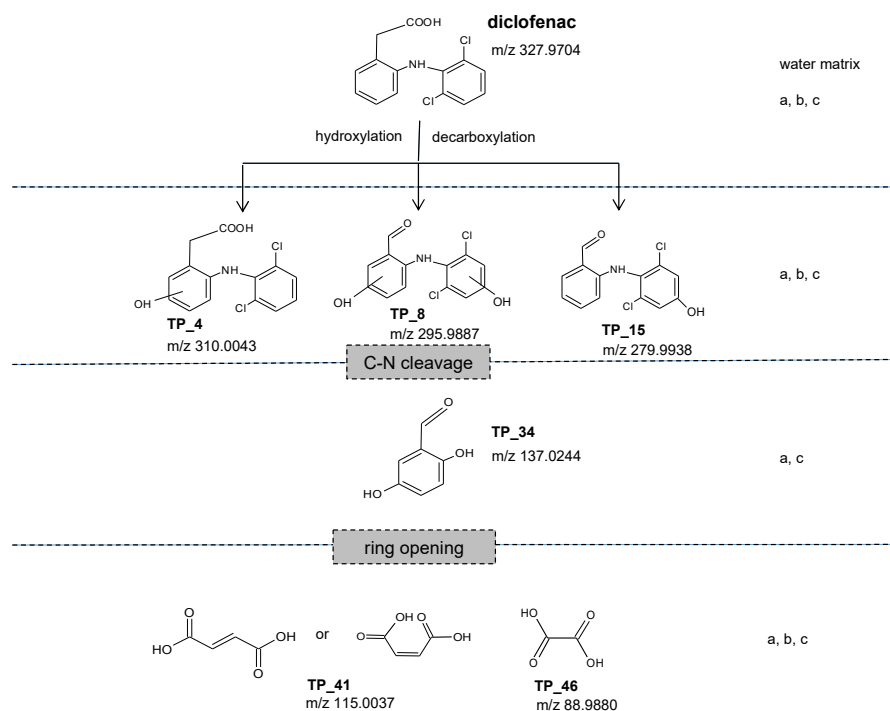


**Figure 2.** Degradation pathway of DCF and the occurrence of identified transformation products (TPs) in the three water matrices: (a) deionized water, (b) drinking water, and (c) wastewater effluent.

Overall, five TPs were identified in all three water matrices at a current density of 292 mA/cm<sup>2</sup>. These contain three structures with two aromatic rings, derived from hydroxylation or decarboxylation of the original compound DCF. Further oxidation leads to the formation of 2,5-dihydroxybenzaldehyde (TP\_34), a one-ring molecule derived from cleavage of the carbon-nitrogen (C–N) bond. This TP could be identified in deionized and drinking water, but not in the wastewater effluent. Two linear structures were also found in all three water matrices: a mixture of maleic acid and fumaric acid (TP\_41), and one product identified as oxalic acid (TP\_46). Thus, DCF was almost degraded to the point of mineralization. For further details, see Supplementary Table S1.

Time courses of the formation and degradation of representative TPs are displayed in Figure 3, as percentages of the peak areas in relation to the respective maximum peak area over the applied charge per volume.

For all water matrices, early-stage TPs containing two aromatic rings appeared in the initial phase of the treatment process. In deionized water, the primary TP 5-hydroxy-DCF (TP\_4) was formed directly after initiation of the oxidation with, a maximum yield after approximately 100 mAh/L, and a complete degradation after 420 mAh/L (Figure 3a), whereas in drinking water and wastewater effluent it took almost 200 mAh/L to reach the maximum yield (Figure 3b,c).

In wastewater effluent, small amounts of 5-hydroxy-DCF could still be detected even after oxidation for 1400 mAh/L. For all water matrices, the increase and decline of the formation of the two other two-ring TPs was slightly delayed compared to 5-hydroxy-DCF. This might be due to the decarboxylation step additional to the hydroxylation.

The one-ring structure 2,5-dihydroxybenzaldehyde was detected at its maximum ratio at 200 mAh/L in deionized water, and was almost fully degraded at 640 mAh/L. In drinking water, the maximum of the curve was reached after 637 mAh/L, and only slightly declined when the oxidation was terminated after 1285 mAh/L. This TP could not be detected in the wastewater effluent. Thus, in the more complex water matrix (wastewater effluent), under the applied conditions, the formation of early-stage DCF TPs with two aromatic rings might be preferred.

During extended oxidation, further ring opening resulted in the formation of the small and highly oxidized molecules fumaric acid and maleic acid/oxalic acid (TP\_41 and TP\_46). In deionized water, the linear TP oxalic acid appeared after 200 mAh/L, and increased in its signal even when the reactor was turned off after 644 mAh/L. A similar behavior could be observed in the more complex water matrices, where small amounts of oxalic acid were already noticed after brief oxidation, and a significant and consistent increase was noticed after 200–300 mAh/L. Even after 1400 mAh/L, the maximum yield was not reached for this molecule. Oxalic acid is reported to be the final product in ozone oxidation, as its reaction with ozone is very slow, whereas the rate constant of the oxidation with hydroxyl radicals is in the region of  $10^7 \text{ m}^{-1}\text{s}^{-1}$  [56]. The presence of this compound even after a longer treatment time indicates that the predominant oxidant present in the solution might be ozone rather than hydroxyl radicals. Thus, under the applied electrode conditions, the target compound DCF was almost mineralized. The second linear product, maleic acid/fumaric acid, could be successfully degraded in all water matrices (for further details, see Supplementary Figure S1).

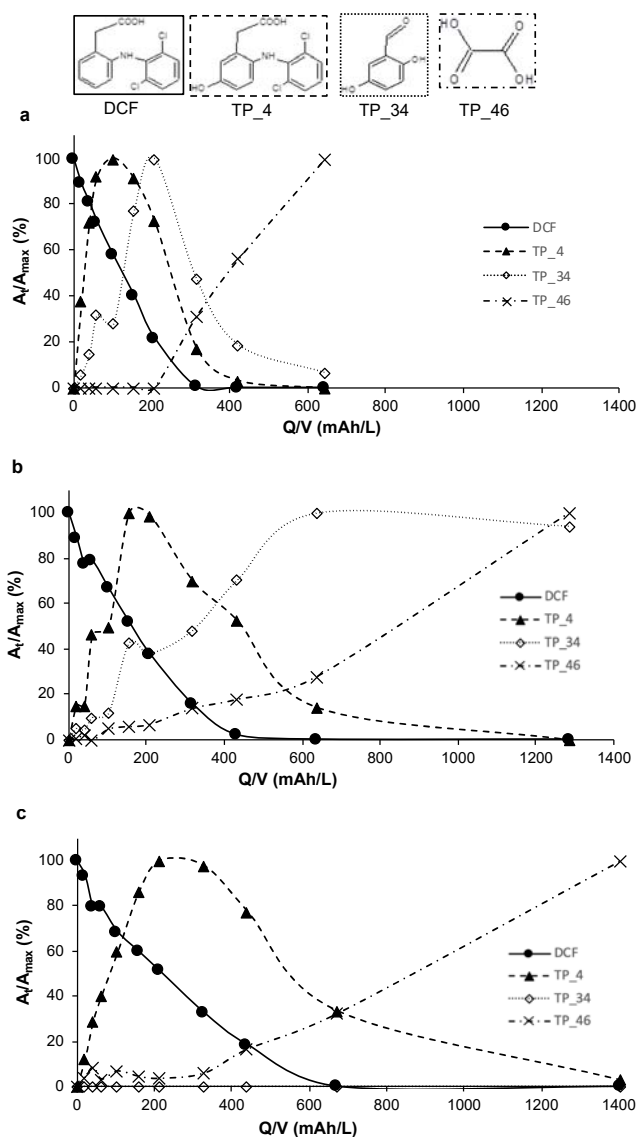


**Figure 3.** Formation and degradation of DCF TPs expressed as %-variation of the peak area of the respective EIC over the applied charge per volume ( $Q/V$ ) in deionized water (a), drinking water (b), and wastewater effluent (c) at  $292 \text{ mA/cm}^2$ .

Determination of the ozone values during the oxidation process supported these findings, since the ozone values exponentially increased up to 1.81 mg/L in deionized water after the majority of the TPs were degraded (after 400 mAh/L). After the electrode was turned off, still no plateau value, and therefore no saturation, was reached for ozone.

The formation and degradation of the five DCF TPs common in the three water matrices was further investigated by varying electrode settings ( $j = 42, 167$  and  $292 \text{ mA/cm}^2$ ). Formation and degradation of the detected TPs were comparable for the applied current densities, with a lower maximum charge per volume input for 42 and  $167 \text{ mA/cm}^2$  compared to  $292 \text{ mA/cm}^2$ . In general, application of the lowest current density resulted in the detection of only a few TPs in each water matrix, as a result of low oxidant production rates. In deionized water, the charge input during the oxidation process generated three primary TPs with two-ring structures. By increasing the current density, the overall number of detected structures, as well as the oxidation state, was enlarged, and degradation of the TPs could also be observed.

As structures with greater oxidation states, such as small linear molecules, require a certain charge input, such TPs were instead formed at higher current densities. In deionized water, fumaric acid/maleic acid and oxalic acid could only be detected at  $292 \text{ mA/cm}^2$ . Application of  $42 \text{ mA/cm}^2$  in the wastewater effluent resulted in a single TP, whereas the same electrode condition in drinking water generated four molecules, including hydrobenzoic acid and fumaric acid/maleic acid. In wastewater effluent, high concentrations of hydrogen bicarbonate preferentially scavenged hydroxyl radicals, whereas organic compounds also reacted with the radicals. Instead, oxalic acid could not be detected at 42 and  $167 \text{ mA/cm}^2$  in any treated water matrices. As reported before, these short-chain organic acids can be easily biodegraded, in contrast with the original compound [12].

### 3.3. Inorganic By-Product Formation

Another aspect of electrochemical water treatment is the formation of inorganic by-products, resulting from oxidation reactions in the presence of chloride and bromide. These oxidation products, such as bromate, perbromate, chlorate or perchlorate, carry a potential health risk [50,57–59].

The experiments focused on the time-dependent formation of the oxohalogenides bromate and chlorate, as well as their peroxo-compounds, in the three water matrices containing varying concentrations of chloride and bromide. Quantitative analysis of bromide and chloride, and the oxidation products chlorate and perchlorate, was performed using ion chromatography analysis (Table 2).

**Table 2.** Concentrations of chloride, bromide, chlorate and perchlorate, derived from IC analysis in deionized water, drinking water and wastewater effluent.

j (mA/cm <sup>2</sup> )	Deionized Water					Drinking Water					Wastewater Effluent				
	Q/V (mAh/L)	Br <sup>-</sup> (mg/L)	Cl <sup>-</sup> (mg/L)	ClO <sub>3</sub> <sup>-</sup> (mg/L)	ClO <sub>4</sub> <sup>-</sup> (mg/L)	Q/V (mAh/L)	Br <sup>-</sup> (mg/L)	Cl <sup>-</sup> (mg/L)	ClO <sub>3</sub> <sup>-</sup> (mg/L)	ClO <sub>4</sub> <sup>-</sup> (mg/L)	Q/V (mAh/L)	Br <sup>-</sup> (mg/L)	Cl <sup>-</sup> (mg/L)	ClO <sub>3</sub> <sup>-</sup> (mg/L)	ClO <sub>4</sub> <sup>-</sup> (mg/L)
42						0	0.989	233	<0.5	<1	0	<0.5	186	<0.5	<1
						14.6	0.898	219	0.709	<1	29.9	<0.5	184	0.913	<1
						29.9	0.841	215	1.12	1.26	95.3	<0.5	176	2.61	2.34
						195	0.406	214	8.63	8.15	199	<0.5	175	5.95	4.96
167						0	1.05	234	<0.5	<1	0	<0.5	186	<0.5	<1
						58.8	0.911	219	0.987	2.35	121	<0.5	176	1.25	2.50
						120	0.825	221	1.79	4.59	380	<0.5	170	4.07	8.18
						375	0.616	218	5.55	17.7	791	<0.5	167	9.40	19.6
292	0	<0.05	0.096	<0.05	<0.1	0	1.06	239	<0.5	<1	0	<0.5	186	<0.5	<1
	101	<0.05	0.794	<0.05	0.115	102	0.818	222	1.08	4.07	214	<0.5	185	1.82	4.55
	207	<0.05	1.50	<0.05	0.218	208	0.703	222	1.86	11.7	674	<0.5	177	5.59	16.9
	644	<0.05	3.10	0.108	0.921	637	0.541	215	6.55	26.3	1403	<0.5	169	11.9	30.0

The detection limits for the inorganic by-products increased ten-fold when using deionized water instead of the more complex water matrices containing high chloride concentrations. Bromate and perbromate could not be detected with IC.

In order to receive more robust data regarding those by-products, a semi-quantitative analysis on the formation of bromate and perbromate, as well as chlorate and perchlorate, could be performed by RPLC-HILIC-MS, and this could also be done in those cases where the respective concentrations for chlorate and perchlorate were below the detection limit of the IC analysis. The formation of inorganic by-products is presented in Figure 4, and the chromatograms of bromate, perbromate, chlorate and perchlorate, obtained from the drinking water matrix, can be found in Supplementary Figure S2.

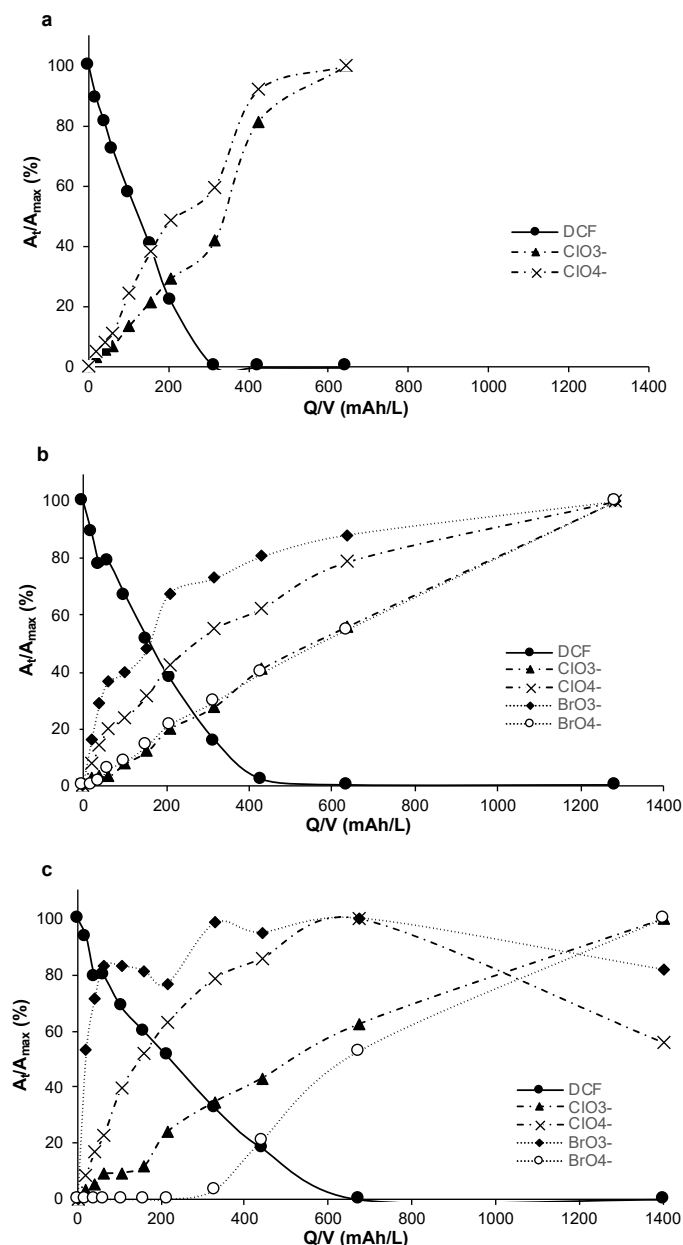


**Figure 4.** Formation of inorganic by-products during DCF degradation as derived from RPLC-HILIC-MS analysis in deionized water (a), drinking water (b), and wastewater effluent (c) at 292 mAh/cm<sup>2</sup>.

RPLC-HILIC-MS data revealed that chlorate was quickly formed in the initial phase, whereas perchlorate increased only slightly (Figure 4a). After approximately 60 mAh/L, chlorate formation reached an almost steady state, which was maintained until the complete degradation of DCF. Perchlorate formation strongly increased after the initial phase, resulting in a higher formation rate for perchlorate compared to chlorate. The highest concentrations were reached after 644 mAh/L, with a maximum of 0.108 mg/L for chlorate and 0.921 mg/L for perchlorate, as derived from the IC data.

Chlorate and perchlorate formation strongly depends on the presence of hydroxyl radicals [60,61]. Thus, compared to the more complex water matrices, relatively high amounts of perchlorate can originate in a water matrix with less radical scavenging molecules. Similarly, in the absence of bromide, formation of the oxidation products bromate and perbromate could not be observed in deionized water.

In drinking water, brominated by-products were also expected. However, these compounds could not be detected quantitatively with IC analysis. As a result of the RPLC-HILIC-MS analysis, those oxidation products could be identified as well, and the signal of chlorate and perchlorate was about 1000-fold higher than that of bromate and perbromate (Figure S2). Initially, there was a strong increase in the bromate curve, which flattened after approximately 60 mAh/L. Chlorate values increased constantly, similar to perbromate, and were always lower than those of bromate and perchlorate (Figure 4b).

A reduction of perchlorate was observed when the current density was decreased (Table 1). As the stepwise oxidation of chloride to perchlorate is driven by hydroxyl radicals, this effect can be explained via the increase of hydroxyl radicals in direct proximity to the electrode at higher current densities, which favors the formation of perchlorate as the highest oxidation state of chloride [59–61]. Other data from the literature also confirm these findings [50,57,62].

In wastewater effluent, the formation of chlorate was comparable to that in drinking water. The ratio of perchlorate to chlorate was remarkably lower, probably resulting from the presence of radical scavenging organic molecules in the wastewater effluent. Even though no bromide and no brominated oxidation products could be detected in the IC analysis, as observed with RPLC-HILIC-MS, bromate formed up to about 80% of its maximum amount immediately upon initiation of the treatment (Figure 4c). Calculated from the peak areas, the estimated amount of bromate was about 1000 times lower than that of chlorate. Perbromate could be detected in traces after 300 mAh/L, with a steady increase afterwards. The formation of brominated oxidation products can occur in the presence of ozone and chlorine in solution [59,63]. Another study reported an inhibition of the bromate formation due to the high chloride concentrations in water [64]. This tendency can be reproduced by comparing the results of the drinking water with the highest chloride content with those of the other water matrices. Overall, the concentrations of the oxidants in wastewater effluent were not sufficient to fully oxidize bromide to perbromate, especially under the condition of high chloride concentrations in the water matrix.

In wastewater effluent, the maximum amounts of chlorate and perchlorate, derived from the IC data, are lower than those in drinking water, considering their concentrations in relation to the treatment time. The measured maximum values are indeed extremely high; however, they result from the long treatment times after the complete removal of DCF and the majority of the early-stage TPs.

Due to their carcinogenic potential, oxidation by-products, such as perchlorate and bromate, must definitely be kept at minimum levels. By legislation, bromate concentrations are limited to a threshold value of 10 µg/L in drinking water according to WHO recommendations [57,63]. Perchlorate discharge is limited to 15 µg/L, according to the US Environmental Protection Agency [65]. In addition, it has to be stressed that in the present study, by adding high concentrations of DCF to the water matrices, the scenario is made to represent the conditions of industrial water treatment.

#### 3.4. Recommended Operating Conditions

The aim of the present study was to investigate the efficiency of BDD in a worst-case scenario (highly contaminated water matrices with increasing complexity), in order to highlight the effects of varied electrode conditions and water composition on the degradation of DCF, and at the same time the formation of TPs as well as inorganic by-products. For this purpose, the concentration of 50 µM DCF was selected based on a comparison with data from the literature [11,66]. The successful removal of persistent pollutants potentially contributes to the elimination of critical molecules from the aquatic environment. However, toxicological and economical aspects have to be considered as well in order to meet the requirements. Thus, the findings may give indications for the optimization of

operating conditions when using BDD electrodes for the removal of persistent chemicals, such as DCF, from a certain water matrix. As a consequence, electrode settings and the extent of treatment should be discussed to achieve optimum conditions.

Through the formation of TPs and oxidation byproducts, an increase in the overall toxicity can certainly not be excluded, and might limit the application of BDD itself. Based on data from the literature, it was reported that metabolites of the initial stage seem to be even more toxic than DCF. Continued oxidation of those compounds quickly reduced this toxicity even further, especially after the complete degradation of the original compound [11,66–68]. Thus, electrochemical treatment should be performed, at least to an extent, where less toxic products and more biodegradable compounds are formed [69], provided no excessive amounts of oxidation by-products are formed. In this instance, the treatment could be executed until the point where about 70% of DCF are degraded. At this stage, the parent compound is removed to a high degree, and at the same time the degradation of early-stage TPs is already in progress. Cleavage of the aromatic ring clearly enhances the biodegradability; some studies even report a positive effect of hydroxylated compounds, as compared to their unsubstituted molecules [70].

On the other hand, at this stage, the amount of inorganic by-products in all water matrices is still very high. Thus, the conducting of the degradation of DCF is recommended only under conditions where by-product formation can be kept at low levels, which requires short treatment times and, at the same time, low current densities. In order to meet the requirements for sufficient DCF removal conditions, the recommendation can be given of operating the electrode using moderate current densities ( $j = 167 \text{ mA/cm}^2$ ), which has sufficient DCF removal efficiency. This is in accordance with data from the literature, which show a clear reduction in bromate, chlorate and perchlorate concentrations when using lower current densities during oxidative water treatment with BDD electrodes [52,57,58,62].

In order to link the data derived from oxidative degradation with economic considerations, the energy expenditure was monitored over the entire treatment process. The total energy demand  $E$  was calculated based on the following Equation (6):

$$E \left( \frac{\text{kWh}}{\text{m}^3} \right) = \frac{E_{\text{cell}} \times I \times T}{V} \quad (6)$$

$E_{\text{cell}}$  is cell voltage (V);  $I$  is applied current (A);  $T$  is treatment time (h); and  $V$  is volume of the treated water ( $\text{m}^3$ ).

The total energy demand of the oxidation reactions during treatment with the BDD electrode in the different water matrices is displayed in Figure 5.

The highest energy consumption in all three water matrices appeared at  $42 \text{ mA/cm}^2$ , as the highest energy demand for the process resulted from the pumping and the control unit. In deionized water, the most advantageous electrode settings appeared at  $167 \text{ mA/cm}^2$  (Figure 5a), whereas in drinking water (Figure 5b) and wastewater effluent (Figure 5c), the highest current density resulted in the lowest energy demand for the treatment process, when considering the total energy.

An explanation can be given by the high content of organic and inorganic compounds in the complex water matrices, resulting in a greater energy demand for the successful oxidation of the target molecule. In this case, the application of lower current densities requires prolonged treatment times and high energetic input. Only a fractional amount of the total energy was consumed by the electrode alone [62]. Thus, electrochemical oxidation using the diamond electrode has the quality of taking place in a competitive range, even for complex water matrices. Decreasing the current densities would also allow the reduction of the overall energy input for the process. However, the applied conditions, and their impact on the process, strongly depend on the water matrix.

An optimization of the reactor geometry and the electrode surface can also contribute to a significant reduction of undesired side effects [31]. It also has to be mentioned that the experiments were performed in batch flow, in a small, laboratory-scale reactor. The results of flow-through experiments in a reactor with a higher throughput will certainly differ considerably from the present

data, particularly with regard to the formation of undesired by-products. Further, different cell types for BDD electrodes have been shown to influence the overall performance, and thus also by-product formation [61].

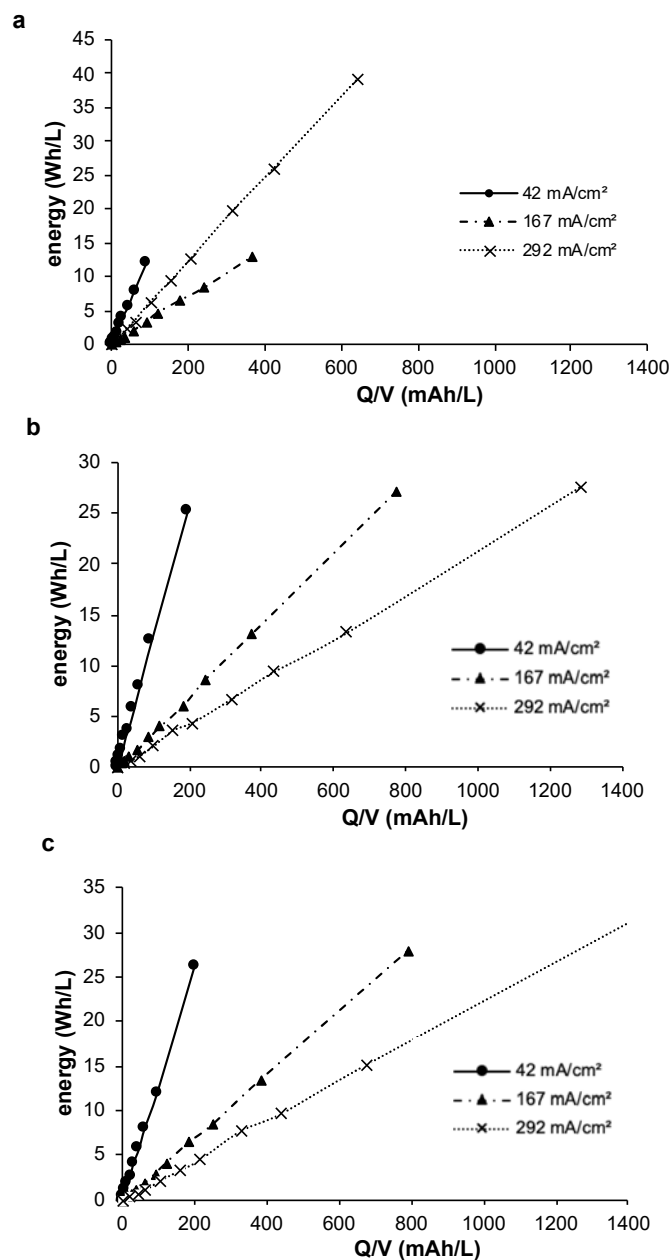


**Figure 5.** Energy demand for oxidation of DCF using different current densities in deionized water (a), drinking water (b) and wastewater effluent (c).

Furthermore, it has to be mentioned that the BDD electrode should rather be considered as an additional treatment step, instead of a stand-alone technology for oxidative water treatment. In this context, it is sufficient to use the electrode up until the initial toxicity is decreased, and the amount of non-degradable compounds is reduced. In subsequent treatment steps, such as bioreactors, sand filters, etc., residual TPs are more accessible to biodegradation, compared to the original compound with relatively low biodegradability [71].

#### 4. Conclusions

Results from the present study revealed that the application of the BDD electrode is effective in the removal of DCF from water matrices of different compositions. As the efficiency of the process depends on the presence of oxidative species, such as ozone and hydroxyl radicals, scavengers for those oxidants present in more complex water matrices, including inorganic and organic constituents, reduce the degradation efficiency. Independent of the water matrix, some early-stage TPs were formed and later degraded again during the treatment process. In addition, the subsequent formation of TPs resulting from cleavage of the aromatic ring systems, as well as small highly oxidized structures, could be identified.

Based on the present data, the aim of this study was to highlight the effects of various electrode settings and the influence of water composition on the degradation process of DCF. Both factors had a major impact on the removal of the original compound, but also on the appearance of TPs, as well as inorganic by-products. Thus, it is necessary to find a balance between successful treatment and toxicological and economic aspects, and to optimize the process in a manner dependent on the composition of the water. Especially in less complex water matrices, the application of relatively low current densities can be sufficient for effective removal of DCF and its TPs. Thereby, by-product formation can clearly be reduced, and at the same time the energy demand can be kept relatively low. Besides the investigation of inorganic by-products and the energy demand, toxicological considerations of the oxidative treatment should also be carried out in the future.

**Supplementary Materials:** The following are available online at <http://www.mdpi.com/2073-4441/12/6/1686/s1>, Figure S1: Formation and degradation curves of DCF TPs expressed as %-variation of the peak area of the respective EIC over the applied charge per volume (Q/V) in deionized water (a), drinking water (b) and wastewater effluent (c) at 292 mA/cm<sup>2</sup>. Figure S2: Extracted ion chromatograms of bromate (m/z 127.9) and perbromate (m/z 143.9) [in (a)]; and chlorate (m/z 83.5) and perchlorate (m/z 99.5) [in (b)], resulting from RPLC-HILIC-MS analysis of drinking water at 292 mA/cm<sup>2</sup>. Table S1: MS data of DCF and six suspected TPs in deionized water (a), drinking water (b) and wastewater effluent (c) after oxidation with 292 mA/cm<sup>2</sup>.

**Author Contributions:** Conceptualization, C.H. and T.L.; methodology, C.H., M.R., G.G. and T.L.; validation, C.H., G.G. and M.R.; formal analysis, G.G. and S.G.; investigation, C.H. and M.R.; data curation, C.H., M.R., G.G. and S.G.; writing—original draft preparation, C.H.; writing—review and editing, T.L., B.H. and J.E.D.; visualization, C.H.; supervision, T.L., B.H. and J.E.D.; project administration, B.H.; funding acquisition, T.L. and B.H. All authors have read and agreed to the published version of the manuscript.

**Funding:** This research was funded by the GERMAN FEDERAL MINISTRY OF EDUCATION AND RESEARCH (BMBF) (03X0087G). This work was supported by the GERMAN RESEARCH FOUNDATION (DFG) and the TECHNICAL UNIVERSITY OF MUNICH (TUM) in the framework of the Open Access Publishing Program.

**Acknowledgments:** G. Greco is grateful to the Foundation BLANCEFLOR Boncompagni-Ludovisi, née Bildt, for financial support. The authors thank Merck Sequant for the column as a gift, and JAS for the HPLC as a loan.

**Conflicts of Interest:** The authors declare no conflict of interest.

#### References

1. Ternes, T.A.; Meisenheimer, M.; McDowell, D.; Sacher, F.; Brauch, H.-J.; Haist-Gulde, B.; Preuss, G.; Wilme, U.; Zulei-Seibert, N. Removal of pharmaceuticals during drinking water treatment. *Environ. Sci. Technol.* **2002**, *36*, 3855–3863. [[CrossRef](#)] [[PubMed](#)]
2. Huber, M.M.; Göbel, A.; Joss, A.; Hermann, N.; Löffler, D.; McArdell, C.S.; Ried, A.; Siegrist, H.; Ternes, T.; von Gunten, U. Oxidation of pharmaceuticals during ozonation of municipal wastewater effluents: A pilot study. *Environ. Sci. Technol.* **2005**, *39*, 8014–8022. [[CrossRef](#)] [[PubMed](#)]
3. Rigobello, E.S.; di Bernardo Dantas, A.; di Bernardo, L.; Vieira, E.M. Removal of diclofenac by conventional drinking water treatment processes and granular activated carbon filtration. *Chemosphere* **2013**, *92*, 184–191. [[CrossRef](#)] [[PubMed](#)]
4. Rossi, L.; Queloz, P.; Brovelli, A.; Margot, J.; Barry, D.A. Enhancement of micropollutant degradation at the outlet of small wastewater treatment plants. *PLoS ONE* **2013**, *8*. [[CrossRef](#)] [[PubMed](#)]

5. Schröder, P.; Helmreich, B.; Škrbić, B.; Carballa, M.; Papa, M.; Pastore, C.; Emre, Z.; Oehmen, A.; Langenhoff, A.; Molinos, M.; et al. Status of hormones and pain killers in wastewater effluents across several European states—Consideration for the EU watch list considering estradiol and diclofenac. *Environ. Sci. Pollut. Res.* **2016**, *2*, 12835–12866. [[CrossRef](#)]
6. Lonappan, L.; Kaur Brar, S.; Kaur Das, R.; Verma, M.; Surampalli, R.Y. Diclofenac and its transformation products: Environmental occurrence and toxicity—A review. *Environ. Int.* **2016**, *96*, 127–138. [[CrossRef](#)]
7. Regnery, J.; Wing, A.D.; Alidina, M.; Drewes, J.E. Biotransformation of trace organic chemical attenuation during groundwater recharge: How useful are first-order rate constants? *J. Contam. Hydrol.* **2015**, *17*, 65–75. [[CrossRef](#)]
8. Sein, M.M.; Zedda, M.; Tuerk, J.; Schmidt, T.C.; Golloch, A.; von Sonntag, C. Oxidation of diclofenac with ozone in aqueous solution. *Environ. Sci. Technol.* **2008**, *42*, 6656–6662. [[CrossRef](#)]
9. Huber, C.; Preis, M.; Harvey, P.J.; Grosse, S.; Letzel, T.; Schröder, P. Emerging pollutants and plants—Metabolic activation of diclofenac by peroxidases. *Chemosphere* **2016**, *146*, 435–441. [[CrossRef](#)]
10. Stülten, D.; Zühlke, S.; Lamshöft, M.; Spittler, M. Occurrence of diclofenac and selected metabolites in sewage effluents. *Sci. Tot. Environ.* **2008**, *405*, 310–316. [[CrossRef](#)]
11. Zhao, X.; Hou, Y.; Liu, H.; Qiang, Z.; Qu, J. Electro-oxidation of diclofenac at boron-doped diamond: Kinetics and mechanism. *Electrochim. Acta* **2009**, *54*, 4172–4179. [[CrossRef](#)]
12. Coelho, A.D.; Sans, C.; Agüera, A.; Gómez, M.J.; Esplugas, S.; Dezotti, M. Effects of ozone pre-treatment on diclofenac: Intermediates, biodegradability and toxicity assessment. *Sci. Total Environ.* **2009**, *407*, 3572–3578. [[CrossRef](#)] [[PubMed](#)]
13. Pérez-Estrada, L.A.; Malato, S.; Gernjak, W.; Agüera, A.; Thurman, E.M.; Ferrer, I.; Fernández-Alba, A.R. Photo-Fenton Degradation of Diclofenac: Identification of main intermediates and degradation pathway. *Environ. Sci. Technol.* **2005**, *39*, 8300–8306. [[CrossRef](#)] [[PubMed](#)]
14. Letzel, M.; Metzner, G.; Letzel, T. Exposure of the pharmaceutical diclofenac based on long-term measurements of the aquatic input. *Environ. Int.* **2009**, *35*, 363–368. [[CrossRef](#)] [[PubMed](#)]
15. European Union Directive 2013/39/EU of the European Parliament and of the Council of 12 August 2013 amending Directives 2000/60/EC and 2008/105/EC as regards priority substances in the field of water policy. *Off. J. Eur. Union* **2013**, *226*, 1–17.
16. Capodaglio, A.G.; Bojanowska-Czajka, A.; Trojanowicz, M. Comparison of different advanced degradation processes for the removal of the pharmaceutical compounds diclofenac and carbamazepine from liquid solutions. *Environ. Sci. Poll. Res.* **2018**, *25*, 27704–27723. [[CrossRef](#)]
17. Menapace, H.M.; Diaz, N.; Weiss, S. Electrochemical treatment of pharmaceutical wastewater by combining anodic oxidation with ozonation. *J. Environ. Sci. Health Part A* **2008**, *43*, 961–968. [[CrossRef](#)]
18. Miklos, D.B.; Remy, C.; Jekel, M.; Linden, K.G.; Drewes, J.E.; Hübner, U. Evaluation of advanced oxidation processes for water and wastewater treatment—A critical review. *Water Res.* **2018**, *77*, 1137–1148. [[CrossRef](#)]
19. Tröster, I.; Schäfer, L.; Fryda, M.; Matthée, T. Electrochemical advanced oxidation process using DiaChem<sup>®</sup> electrodes. *Water Sci. Technol.* **2004**, *49*, 207–212. [[CrossRef](#)]
20. Rivera-Utrilla, J.; Sánchez-Polo, M.; Ferro-García, M.A.; Prados-Joya, G.; Ocampo-Pérez, R. Pharmaceuticals as emerging contaminants and their removal from water. A review. *Chemosphere* **2013**, *93*, 1268–1287. [[CrossRef](#)]
21. Ribeiro, A.R.; Nunes, O.C.; Pereira, M.F.R.; Silva, A.M.T. An overview on the advanced oxidation processes applied for the treatment of water pollutants defined in the recently launched Directive 2013/39/EU. *Environ. Int.* **2015**, *7*, 33–51. [[CrossRef](#)] [[PubMed](#)]
22. Oturan, M.A.; Aaron, J.-J. Advanced Oxidation Processes in Water/Wastewater Treatment: Principles and Applications. A Review. *Crit. Rev. Environ. Sci. Technol.* **2014**, *44*, 2577–2641. [[CrossRef](#)]
23. Rajab, M.; Greco, G.; Heim, C.; Helmreich, B.; Letzel, T. Serial coupling of RP and zwitterionic hydrophilic interaction LC-MS: Suspects screening of diclofenac transformation products by oxidation with a boron-doped diamond electrode. *J. Sep. Sci.* **2013**, *36*, 3011–3018. [[PubMed](#)]
24. Helmreich, B.; Metzger, S. Post-treatment for micropollutants removal. In *Innovative Wastewater Treatment & Resource Recovery Technologies: Impacts on Energy, Economy and Environment*; Lema, J.M., Suarez Martinez, S., Eds.; IWA-Publishing: London, UK, 2017; pp. 2014–2232. ISBN 13: 9781780407869.

25. Brillas, E.; Garcia-Segura, S.; Skoumal, M.; Arias, C. Electrochemical incineration of diclofenac in neutral aqueous medium by anodic oxidation using Pt and boron-doped diamond anodes. *Chemosphere* **2010**, *79*, 605–612. [[CrossRef](#)] [[PubMed](#)]
26. Coria, G.; Nava, J.L.; Carreno, G. Electrooxidation of diclofenac in synthetic pharmaceutical wastewater using an electrochemical reactor equipped with a boron doped diamond electrode. *J. Mex. Chem. Soc.* **2014**, *58*, 303–308. [[CrossRef](#)]
27. Faber, H.; Lutze, H.; Lareo, P.L.; Frensemeier, L.; Vogel, M.; Schmidt, T.C.; Karst, U. Liquid chromatography/mass spectrometry to study oxidative degradation of environmentally relevant pharmaceuticals by electrochemistry and ozonation. *J. Chromatogr. A* **2014**, *1343*, 152–159. [[CrossRef](#)]
28. Vedenyapina, M.D.; Strel'tsova, E.D.; Davshan, N.A.; Vedenyapin, A.A. Study of the electrochemical degradation of diclofenac on a boron doped diamond electrode by UV spectroscopy. *Russ. J. Appl. Chem.* **2011**, *84*, 204–207. [[CrossRef](#)]
29. Frontistis, Z.; Brebou, C.; Venieri, D.; Mantzavinos, D.; Katsaounis, A. BDD anodic oxidation as tertiary wastewater treatment for the removal of emerging micro-pollutants, pathogens and organic matter. *J. Chem. Technol. Biot.* **2011**, *86*, 1233–1236. [[CrossRef](#)]
30. Martínez-Huitle, C.A.; Quiroz Alfaro, M.A. Recent environmental applications of diamond electrode: Critical review. *J. Environ. Eng. Manag.* **2008**, *18*, 155–172.
31. Rajab, M.; Heim, C.; Letzel, T.; Drewes, J.E.; Helmreich, B. Oxidation of bisphenol A by boron-doped diamond electrode in different water matrices: Transformation products and inorganic by-products. *Int. J. Environ. Sci. Technol.* **2016**, *13*, 2539–2548. [[CrossRef](#)]
32. Schmalz, V.; Dittmar, T.; Fischer, D.; Worch, E. Diamond electrodes in decentralized wastewater treatment: Electrochemical degradation of the chemical oxygen demand (COD) in wastewater with high organic loads from hardening shops. *CIT* **2008**, *80*, 1545–1550.
33. Honda, Y.; Ivandini, T.A.; Watanabe, T.; Murata, K.; Einaga, Y. An electrolyte-free system for ozone generation using heavily boron-doped diamond electrodes. *Diam. Relat. Mater.* **2013**, *40*, 7–11. [[CrossRef](#)]
34. Michaud, P.-A.; Panizza, M.; Ouattara, L.; Diaco, T.; Foti, G.; Comninellis, C. Electrochemical oxidation of water on synthetic boron-doped diamond thin film anodes. *J. Appl. Electrochem.* **2003**, *33*, 151–154. [[CrossRef](#)]
35. Panizza, M.; Brillas, E.; Comninellis, C. Application of boron-doped diamond electrodes for wastewater treatment. *J. Environ. Eng. Manag.* **2008**, *18*, 139–153.
36. Lara-Ramos, J.A.; Saez, C.; Machuca-Martínez, F.; Rodrigo, M.A. Electro-ozonizers: A new approach for an old problem. *Sep. Purif. Technol.* **2020**, *241*. [[CrossRef](#)]
37. Von Gunten, U. Ozonation of drinking water: Part I. Oxidation kinetics and product formation. *Water Res.* **2003**, *37*, 1443–1467. [[CrossRef](#)]
38. Calza, P.; Sakkas, V.A.; Medana, C.; Baiocchi, C.; Dimou, A.; Pelizzetti, E.; Albanis, T. Photocatalytic degradation study of diclofenac over aqueous TiO<sub>2</sub> suspension. *Appl. Catal. B-Environ.* **2006**, *67*, 197–205. [[CrossRef](#)]
39. Merel, S.; Lege, S.; Yanez Heras, J.E.; Zwiener, C. Assessment of n-oxide formation during wastewater ozonation. *Environ. Sci. Technol.* **2017**, *51*, 410–417. [[CrossRef](#)]
40. Ternes, T.A.; Prasse, C.; Eversloh, C.L.; Knopp, G.; Cornel, P.; Schulte-Oehlmann, U.; Schwartz, T.; Alexander, J.; Seitz, W.; Coors, A.; et al. Integrated evaluation concept to assess the efficiency of advanced wastewater treatment processes for the elimination of micropollutants and pathogens. *Environ. Sci. Technol.* **2017**, *51*, 308–319. [[CrossRef](#)]
41. Wert, E.C.; Gonzales, S.; Dong, M.M.; Rosario-Ortiz, F.L. Evaluation of enhanced coagulation pretreatment to improve ozone oxidation efficiency in wastewater. *Water Res.* **2009**, *45*, 5191–5199. [[CrossRef](#)]
42. Heim, C.; Ureña de Vivanco, M.; Rajab, M.; Müller, E.; Letzel, T.; Helmreich, B. Rapid inactivation of waterborne bacteria using boron-doped diamond electrodes. *Int. J. Environ. Sci. Technol.* **2015**, *12*, 3061–3070. [[CrossRef](#)]
43. Greco, G.; Grosse, S.; Letzel, T. Serial coupling of reversed-phase and zwitterionic hydrophilic interaction LC/MS for the analysis of polar and nonpolar phenols in wine. *J. Sep. Sci.* **2013**, *36*, 1379–1388. [[CrossRef](#)] [[PubMed](#)]
44. Stadlmair, L.F.; Grosse, S.; Letzel, T.; Drewes, J.E.; Grassmann, J. Comprehensive MS-based screening and identification of pharmaceutical transformation products formed during enzymatic conversion. *Anal. Bioanal. Chem.* **2019**, *411*, 339–351. [[CrossRef](#)] [[PubMed](#)]

45. Baird, R.B.; Eaton, A.D.; Rice, E.W. *Standard Methods for the Examination of Water and Wastewater*, 23rd ed.; American Public Health Association: Washington, DC, USA, 2017.
46. Bader, H.; Hoigné, J. Determination of ozone in water by the indigo method. *Water Res.* **1981**, *15*, 449–456. [[CrossRef](#)]
47. Heim, C.; Ureña de Vivanco, M.; Rajab, M.; Glas, K.; Horn, H.; Helmreich, B.; Letzel, T. Ozone II: Characterization of in situ ozone generation using diamond electrodes. *BrewingScience* **2011**, *64*, 83–88.
48. Bergmann, H.M.E.; Rollin, J.; Iourtchouk, T. The occurrence of perchlorate during drinking water electrolysis using BDD anodes. *Electrochim. Acta* **2009**, *54*, 2102–2107. [[CrossRef](#)]
49. Bergmann, H.M.E.; Rollin, J. Product and by-product formation in laboratory studies on disinfection electrolysis of water using boron-doped diamond electrodes. *Catal. Today* **2007**, *124*, 198–203. [[CrossRef](#)]
50. Polcaro, A.M.; Vacca, A.; Mascia, M.; Ferrara, F. Product and by-product formation in electrolysis of dilute chloride solutions. *J. Appl. Electrochem.* **2008**, *38*, 979–984. [[CrossRef](#)]
51. Lee, Y.; von Gunten, U. Oxidative transformation of micropollutants during municipal wastewater treatment: Comparison of kinetic aspects of selective (chlorine, chlorine dioxide, ferrate VI, and ozone) and non-selective oxidants (hydroxyl radical). *Water Res.* **2010**, *44*, 555–566. [[CrossRef](#)]
52. Polcaro, A.M.; Vacca, A.; Mascia, M.; Palmas, S.; Rodriguez Ruiz, J. Electrochemical treatment of waters with BDD anodes: Kinetics of the reactions involving chlorides. *J. Appl. Electrochem.* **2009**, *39*, 2083–2092. [[CrossRef](#)]
53. Soufan, M.; Deborde, M.; Legube, B. Aqueous chlorination of diclofenac: Kinetic study and transformation products identification. *Water Res.* **2012**, *46*, 3377–3386. [[CrossRef](#)] [[PubMed](#)]
54. Vogna, D.; Marotta, R.; Napolitano, A.; Andreozzi, R.; d’Ischia, M. Advanced oxidation of the pharmaceutical drug diclofenac with UV/H<sub>2</sub>O<sub>2</sub> and ozone. *Water Res.* **2004**, *38*, 414–422. [[CrossRef](#)] [[PubMed](#)]
55. Faber, H.; Melles, D.; Brauckmann, C.; Wehe, C.A.; Wentker, K.; Karst, U. Simulation of the oxidative metabolism of diclofenac by electrochemistry/(liquid chromatography)/mass spectrometry. *Anal. Bioanal. Chem.* **2012**, *403*, 345–354. [[CrossRef](#)] [[PubMed](#)]
56. Gandini, D.; Mahé, E.; Michaud, P.A.; Haenni, W.; Perret, A.; Comninellis, C. Oxidation of carboxylic acids at boron-doped diamond electrodes for wastewater treatment. *J. Appl. Electrochem.* **2000**, *30*, 1345–1350. [[CrossRef](#)]
57. Bergmann, H.M.E.; Iourtchouk, T.; Rollin, J. The occurrence of bromate and perbromate on BDD anodes during electrolysis of aqueous systems containing bromide: First systematic experimental studies. *J. Appl. Electrochem.* **2011**, *41*, 1109–1123. [[CrossRef](#)]
58. Palmas, S.; Polcaro, A.M.; Vacca, A.; Mascia, M.; Ferrara, F. Influence of the operating conditions on the electrochemical disinfection process of natural waters at BDD electrodes. *J. Appl. Electrochem.* **2007**, *37*, 1357–1365. [[CrossRef](#)]
59. Von Gunten, U. Ozonation of drinking water: Part II. Disinfection and by-product formation in presence of bromide, iodide or chlorine. *Water Res.* **2003**, *37*, 1469–1487. [[CrossRef](#)]
60. Sánchez-Carretero, A.; Sáez, C.; Cañizares, P.; Rodrigo, M.A. Electrochemical production of perchlorates using conductive diamond electrolyses. *Chem. Eng. J.* **2011**, *166*, 710–714. [[CrossRef](#)]
61. Isidro, J.; Brackemeyer, D.; Sáez, C.; Llanos, J.; Lobato, J.; Cañizares, P.; Matthée, T.; Rodrigo, M.A. Testing the use of cells equipped with solid polymer electrolytes for electro-disinfection. *Sci. Total Environ.* **2020**, *725*. [[CrossRef](#)]
62. Rajab, M.; Heim, C.; Letzel, T.; Drewes, J.E.; Helmreich, B. Electrochemical disinfection using boron-doped diamond electrode—The synergetic effects of in situ ozone and free chlorine generation. *Chemosphere* **2015**, *121*, 47–53. [[CrossRef](#)]
63. Heeb, M.B.; Criquet, J.; Zimmermann-Steffens, S.G.; von Gunten, U. Oxidative treatment of bromide-containing waters: Formation of bromine and its reactions with inorganic and organic compounds—A critical review. *Water Res.* **2014**, *48*, 15–42. [[CrossRef](#)] [[PubMed](#)]
64. Vacca, A.; Mascia, M.; Palmas, S.; Mais, L.; Rizzardini, S. On the formation of bromate and chlorate ions during electrolysis with boron-doped diamond anode for seawater treatment. *J. Chem. Technol. Biotechnol.* **2013**, *88*, 2244–2251. [[CrossRef](#)]
65. Bergmann, M.E.H.; Korparal, A.S.; Iourtchouk, T. Electrochemical advanced oxidation processes, formation of halogenate and perhalogenate species—A critical review. *Crit. Rev. Environ. Sci. Technol.* **2014**, *44*, 348–390. [[CrossRef](#)]

66. Bojanowska-Czajka, A.; Kciuk, G.; Gumiela, M.; Borowiecka, S.; Nalecz-Jawecki, G.; Koc, A.; Garcia-Reyes, J.F.; Solpan Ozbay, D.; Trojanowicz, M. Analytical, toxicological and kinetic investigation of decomposition of the drug diclofenac in waters and wastes using gamma radiation. *Environ. Sci. Pollut. Res.* **2015**, *22*, 20255–20270. [[CrossRef](#)] [[PubMed](#)]
67. Diniz, M.S.; Salgado, R.; Pereira, V.J.; Carvalho, G.; Oehmen, A.; Reis, M.A.M.; Noronha, J.P. Ecotoxicity of ketoprofen, diclofenac, atenolol and their photolysis byproducts in zebrafish (*Danio rerio*). *Sci. Total Environ.* **2015**, *505*, 282–289. [[CrossRef](#)] [[PubMed](#)]
68. Yu, H.; Nie, E.; Xu, J.; Yan, S.; Cooper, W.J.; Song, W. Degradation of Diclofenac by Advanced Oxidation and Reduction Processes: Kinetic Studied, Degradation Pathways and Toxicity Assessments. *Water Res.* **2013**, *47*, 1909–1918. [[CrossRef](#)]
69. Martínez-Huitle, C.A.; Ferro, S.; de Battisti, A. Electrochemical incineration of oxalic acid: Reactivity and engineering parameters. *J. Appl. Electrochem.* **2005**, *35*, 1087–1093. [[CrossRef](#)]
70. Hübner, U.; von Gunten, U.; Jekel, M. Evaluation of the persistence of transformation products from ozonation of trace organic compounds—A critical review. *Water Res.* **2015**, *68*, 150–170. [[CrossRef](#)]
71. Liwarska-Bizukojc, E.; Galamon, M.; Bernat, P. Kinetics of Biological Removal of the Selected Micropollutants and Their Effect on Activated Sludge Biomass. *Water Air Soil Pollut.* **2018**, *229*, 356. [[CrossRef](#)] [[PubMed](#)]



© 2020 by the authors. Licensee MDPI, Basel, Switzerland. This article is an open access article distributed under the terms and conditions of the Creative Commons Attribution (CC BY) license (<http://creativecommons.org/licenses/by/4.0/>).